Chapter 3: Spatiotemporal Self-Organization on a Pt Ring Electrode in Bi-enhanced HCOOH oxidation (Galvanostatic Conditions)

3.1 Introduction

The occurrence of dynamic instabilities in electrochemical reactions has been studied for a long time [47, 48, 50, 52, 61-66]. These researches made substantial advances in the understanding of such self-organized inhomogeneous spatial variations of interfacial potential near the electrochemical interface. While earlier studies evidenced pattern formation of inhomogeneous interfacial potential in electrodissolution reaction [11, 67-70], the research has been recently addressing pattern formations in electrocatalytic oxidation reactions, and experimental electrocatalysis in a spatiotemporally inhomogeneous oscillating regime has well reported [14, 18-20, 71].

Pattern formation in electrochemical systems occurs at the electrode/electrolyte interface and results from the interplay between interfacial kinetics and transport processes parallel to the electrolyte surface. Flätgen and Krischer [12, 17, 72] have studied the spatiotemporal phenomena that accompany the transition between two stable states or the oscillations during the peroxodisulfate ($S_2O_8^{2-}$) reduction at a Ag ring or disk electrode. They found that the transition from one state to the other was meditated by fronts at the electrode. Mazouz *et al*. [73, 74] found that the range of the coupling depended crucially on the length scale of the system, *i.e.*, the real size of the working electrode and the equipotential plane provided by the counter or reference electrode, and that the strength of the coupling was proportional to the conductivity of the electrolyte. Long-ranged coupling

brought about by a small electrode area or a long distance to the reference electrode has the tendency to synchronize the events on the electrode surface. Very short-ranged coupling results in 'ordinary' reaction-diffusion behavior, and leads to waves of constant velocity. The intermediate range of 'nonlocal' coupling leads to the accelerating fronts. In the oscillatory regime, nonlocal coupling may lead to destabilization of the homogeneous oscillation mode and torus-like or irregular oscillations of the overall current may develop owing to the superposition of the homogeneous oscillation and various types of standing waves on the surface.

As already discussed in chapter 1, reaction-migration formalism [34, 67] presented a theoretical and numerical description of pattern formation in electrochemistry. Assuming the validity of the Laplace equation within the electrolyte, potential theory leads to the differential equation for the description of the evolution of the interfacial potential across the working electrode. The equation for the interfacial potential consisted of the local faradaic reaction terms describing the chemical reaction, the local coupling included migration current, and an integral term according for the spatial migration coupling parallel to the electrified interface. The integral involved a spatial migration coupling function indicating the sign and strength of the coupling between two different points in the electrode. In the potentiostatic condition, migration coupling along the electrode was affected by the geometry of the electrochemical cell, especially the relative position of the working and reference electrode. If the reference electrode is close to the working electrode, negative nonlocal migration coupling leads to inhomogeneties of the interfacial potential. Positive nonlocal migration coupling favors synchronization of the interfacial potential if the reference electrode is far away from the working electrode [71]. In the symmetric electrode geometry, the whole surface of working electrode is affected equally by the reference electrode.

The oxidation of formic acid on Pt in the presence of foreign ad-atoms was studied by many researchers and the catalytic activity of bismuth modified Pt in the oxidation of formic acid has greater effects than other ad-atoms [75-77]. Bismuth modification of the Pt electrode can increase the reaction of formic acid oxidation according to the bismuth coverage [78, 79] and temperature [80].

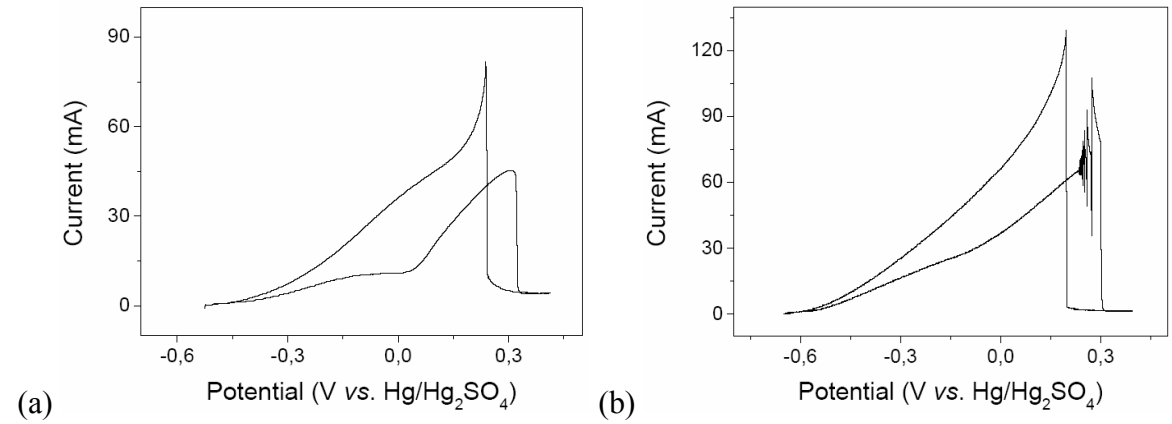

Figure 3.1. Cyclic voltammetry of electro-oxidation of formic acid on a Pt ring electrode in the absence of Bi^{3+} ions (a) and in the presence of Bi^{3+} (1×10^{-6} M) ions (b). Electrolyte is 0.1 M HCOONa / 0.033 M H_2SO_4 and scan rate is 10 mV/s.

Figure 3.1(a) displays a cyclic voltammetry of electro-oxidation of formic acid on a Pt ring electrode in the absence of Bi ions. On the anodic scan, the direct formic acid oxidation occurred on sites not blocked by CO in the absence of considerable of amount of oxygen-containing species. At more anodic potential, CO became gradually removed giving way to high rate of direct formic acid oxidation (active state). More anodically, oxygen-containing species poisoned the surface and deactivated the electrode. Upon turning the potential scan, the electrode remained deactivated (passive state). The system then entered the bistable regime (active and passive state coexisting) until at more cathodic potential a sudden desorption of the poisoning species occurred which brought the system back on the active branch of the cyclic voltammetry. In the presence of Bi^{3+} ions, in Figure 3.1(b), activated state changed to the current oscillatory regime before the passive transition on anodic scan.

In the oscillatory regime, Figure 3.1(b), various spatiotemporal pattern formation could be observed with close RE. At low anodic potential within the oscillatory regime (+0.20 V), period-1 current oscillations and standing wave pattern formation were shown clearly in Figure 3.2(a) and (b). The potential distribution along one half of the ring electrode was shifted by 180° relative to the other half of the electrode. After showing the standing wave pattern formation, at more anodic potential (+0.22 V), a travelling pulse

wave can be observed clearly in Figure 3.3. During period-2 current oscillations in Figure 3.3(a), active (blue; low interfacial potential) and passive (red: high interfacial potential) pulses were travelling continuously with constant velocity in Figure 3.3(b).

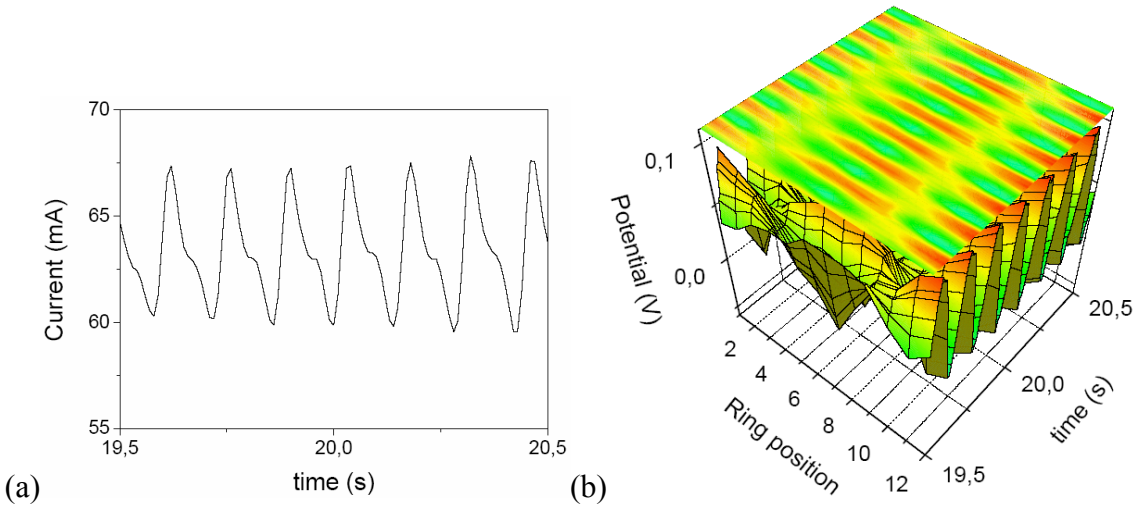

Figure 3.2. (a) Current oscillations and (b) spatiotemporal pattern formation of standing wave at +0.20 V.

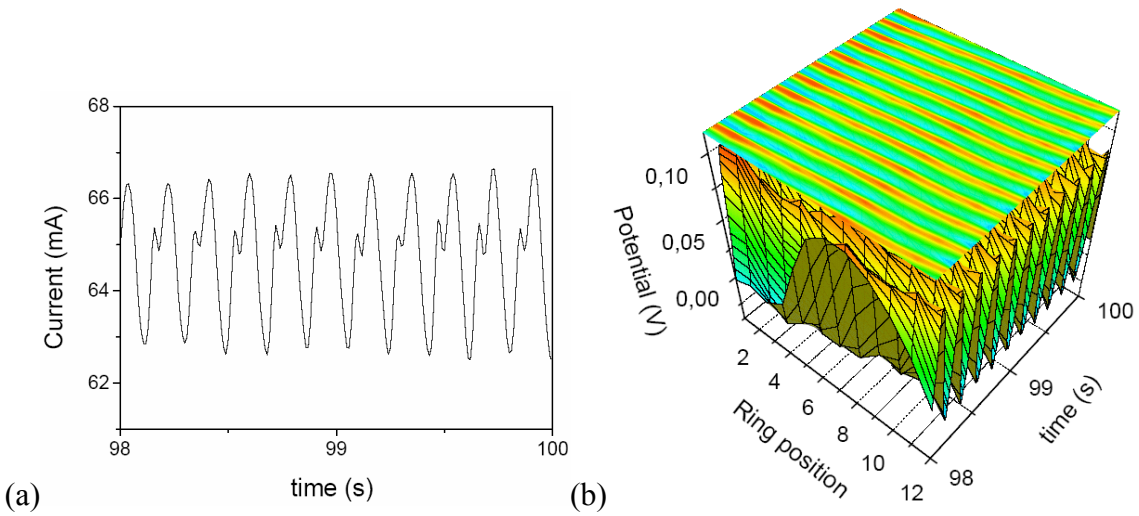

Figure 3.3. (a) Current oscillations and (b) spatiotemporal pattern formation of travelling pulse wave at +0.22 V.

Chaos, including well-defined transitions to chaos, has been observed numerous times in electrochemistry. In fact as earlier as 1900 Ostwald [4] reported electrochemical oscillations which indicate chaos (though the term had not been coined at the time, and the published time series are too short to allow an unambiguous decision). Considerably later, numerous studies showed the emergence of chaos in metal dissolution. Diem and Hudson [81] showed the existence of simple and higher order chaotic oscillations during the electrodissolution of Fe in H_2SO_4 at the limiting current plateau. Cu electrodissolution in H_3PO_4 has been studied by Albahadily and Schell [82] and has been found to undergo Hopf bifurcations to oscillatory behavior and period-doubling bifurcations to simple chaos. Lev *et al*. have reported a saddle loop bifurcation, period-doubling bifurcation, chaos, and quasi-periodicity [83]. Bassett and Hudson [84, 85] have shown that Cu electrodissolution in NaCl and H_2SO_4 gives a plethora of interesting behavior, including a variety of periodic oscillations, period-2, type III intermittency, windows of period-3 oscillations within chaotic regions, and *Shil'nikov* chaos. Chaotic oscillations in electro-oxidation reactions have been found also, *e.g.*, in formaldehyde, methanol, ethanol ethylene glycol, and glycerol [48, 71, 75-77, 86-94].

Here we investigated the potential oscillations in formic acid oxidation with bismuth ions. In particular we studied the transition from periodic potential oscillations to *Shil'nikov* chaotic potential oscillations at fixed current.

3.2 Experimental

The schematic view of the experimental setup is shown in Figure 3.4. A smooth polycrystalline Pt ring with inner diameter of 34 mm and outer diameter of 40 mm (thus exhibiting a geometric surface area of *ca*.7 cm^2) was used as the working electrode (WE). A concentric platinized Pt wire ring (thickness of 1 mm wire, 220 mm ring circumference) used as counter electrode (CE) was placed 80 mm above the working electrode. The tip of a Luggin-Haber capillary hosting a Hg/Hg_2SO_4, K_2SO_4 (sat'd) reference electrode (RE) was positioned the center of the ring WE.

To detect the instantaneous local surface potentials on the Pt ring electrode, twelve microprobes were placed along the ring electrode close to the electrode surface (0.2 mm).

Each microprobe capped with the Hg/Hg_2SO_4 electrode was filled with a 0.5 M Na_2SO_4 solution (Merck, p.a.) [21]. All solutions were prepared with ultrapure water (Millipore Milli-Q water, 18 MΩ·cm) and were kept at room temperature. Before each experiment, the Pt ring electrode was chemically cleaned. For investigation of the electrocatalytic oxidation of formic acid, 0.1 M HCOONa (Merck, p.a.) in 0.033 M H_2SO_4 was used as the electrolyte. Bismuth ions (Bi^{3+}) were prepared from Bi_2O_3 (Strem Chemicals Inc.) which was dissolved in 0.5 M $HClO_4$ (Merck, suprapure) [95]. The electrolyte was extensively bubbled with N_2 before each experiment. A nitrogen atmosphere was maintained over the unstirred solutions during sweep experiments. Galvanostatic scan and constant current methods (effect of formic acid concentration by using reaction time) were executed with a bi-potentiostat (Model 366, EG&G). In an unstirred solution, the HCOOH concentration near the WE will slowly decrease over time. This effect was used as a slow parameter drift in order to determine the bifurcation scenario (1-parameter cut). Such runs could typically be repeated 3-4 times by magnetically stirring the electrolyte for 1 min, restoring the initial HCOOH concentration at the WE and restarting the drift after switching off the stirrer. After several hours other effects (probably poisoning of the WE by impurities) hampered reproducibility, and the experiment had to be restarted after cleaning the electrode with the procedure described above.

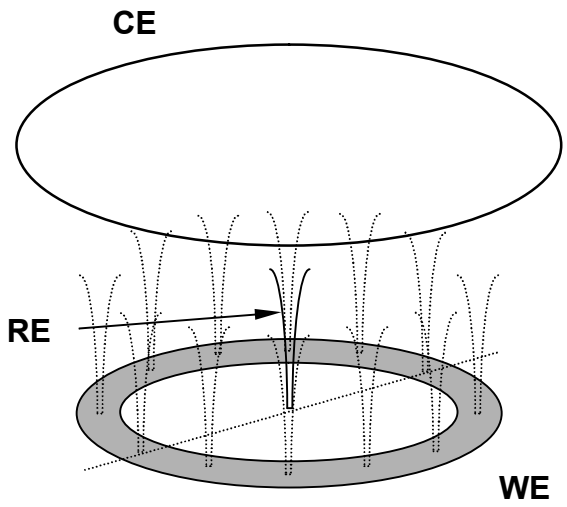

Figure 3.4. Schematic view of the electrode setup. Reference electrode (RE) is placed into the center of a Pt ring electrode (WE). Counter electrode (CE) situates above the plane of WE. Twelve potential microprobes are separated by 30° angles.

3.3 Results

3.3.1 Effects of bismuth ions on oxidation of formic acid

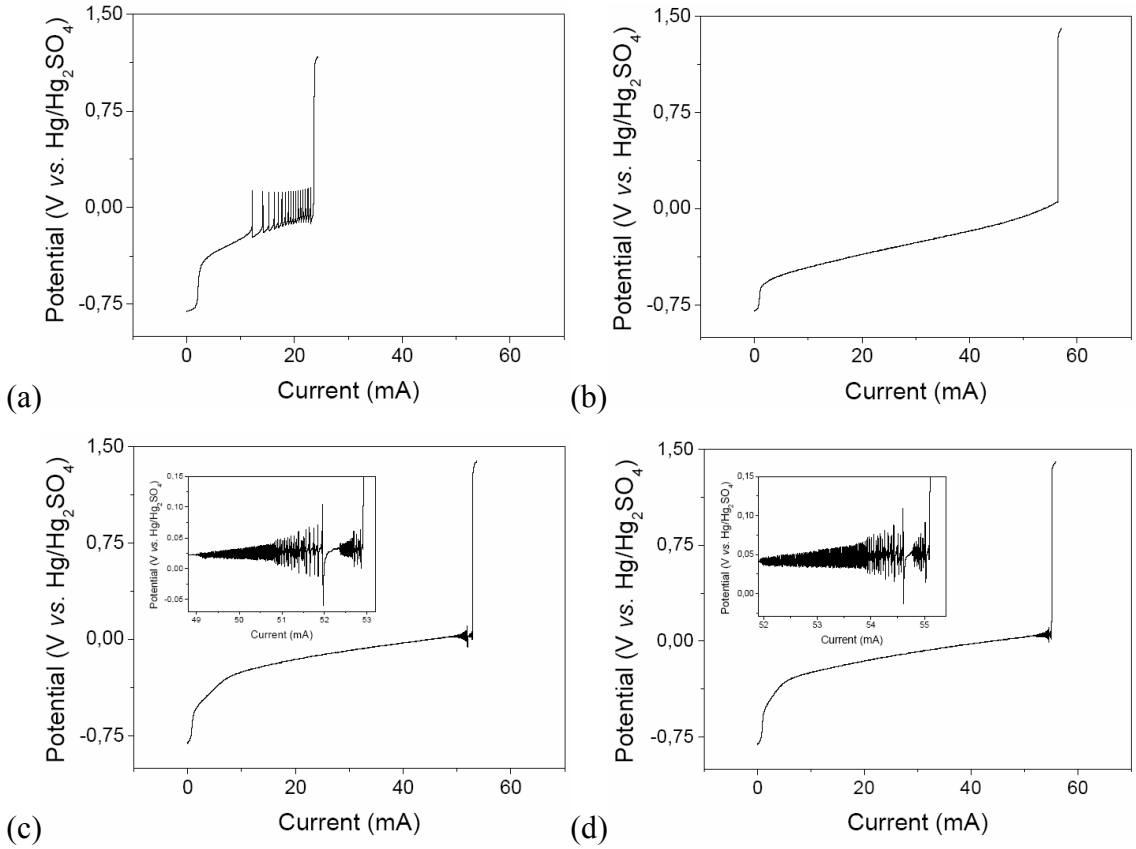

Figure 3.5. Voltage is plotted against current during the oxidation of formic acid in 0.1 M HCOONa / 0.033 M H_2SO_4 in galvanostatic system. (a) without bismuth ions, (b) 1×10^{-7} M, (c) 5×10^{-7} M and (d) 1×10^{-6} M bismuth ions. Scan rate 0.1 mA/s.

Figure 3.5 shows the different potential-current profiles on oxidation of formic acid in 0.1 M HCOONa / 0.033 M H_2SO_4 solution according to the absence or the existence of the bismuth ions during a galvanostatic current scan of 0.1 mA/s. In the absence of bismuth ions, large amplitude and low frequency of potential oscillations were observed in Figure 3.5(a) [93, 94]. Potential oscillations were shown up to +23.38 mA which was the maximum current before the potential changed to the very large value (overshoot of potential) to +1.15 V. With small amount of bismuth ions, 1×10^{-7} M, potential oscillations did not occur in Figure 3.5(b). When we added 5×10^{-7} M bismuth ions to the above solution,

different potential oscillations which had high frequency were observed over a larger current range and the overshoot of potential to +1.31 V occurred at the current +53.02 mA in Figure 3.5(c). Increasing the concentration of bismuth ions to 1×10^{-6} M, the current range of occurring potential oscillations and overshoot of potential was more extended in Figure 3.5(d). An overshoot of potential to +1.35 V occurred at the current +55.29 mA and high frequency and various forms of potential oscillations were obtained also.

When adding the bismuth ions to the solution, we could get a low potential value over a large current range. In other words, bismuth enhanced the oxidation of formic acid at low potential values. The current at the point of the overshoot of potential was increased, which means that the stationary state of potential was stable at the large current value [92]. In the enlargement of Figure 3.5(c) and (d), potential oscillations had various forms on increasing current range when the bismuth ions were used in the oxidation of formic acid. In low current range, period-1 potential oscillations were observed. As the current increased, potential oscillations were changed to period-2 and at last became aperiodic before the potential was overshoot. The detailed potential oscillations will be subsequently discussed.

3.3.2 Period doubling and experimental approach to a *Shil'nikov* orbit

To get the various and long term potential oscillations of formic acid oxidation, we studied the potential oscillations under the chronopotentiometric condition. Various potential oscillation patterns are shown in Figure 3.6, which is the result of formic acid oxidation in 0.1 M HCOONa / 0.033 M H_2SO_4 with bismuth ions solution at the fixed current of +53 mA. At the beginning of potential oscillations, period-1 oscillations with small amplitude arose, Figure 3.6(a). With passing reaction time, period-2 oscillations took place; small and large amplitude of potential alternate, Figure 3.6(b). Before the period-2 oscillations changed to the aperiodic potential oscillations, the second period-doubling bifurcation gave rise to a period-2^2 pattern for a short time, as shown in the dotted box of Figure 3.6(b) which is characteristic of the Feigenbaum route to chaos [96]. After some reaction time, the oscillations became aperiodic (type I) in Figure 3.6(c), although still confined to relatively narrow amplitude of a potential range about +0.1 V. After yet longer times, a qualitative change of the aperiodic behavior was observed; the small-amplitude irregular oscillations became interrupted by bursts with large amplitudes (type II). These

excursion occurred in irregular intervals, whereby these intervals became longer with further passing of reaction time, Figure 3.6(d)-(f). The transient observation of period-doubled behavior indicates the continued existence of unstable periodic orbits from the Feigenbaum scenario.

Further characterization of this state was obtained from a construction of the associated three-dimensional attractors (through the time-delay method). The period-1 potential oscillations had a simple attractor which was one closed line (Figure 3.7(a)) and the period-2 potential oscillations had two closed line, Figure 3.7(b). Aperiodic oscillations after the period-2 oscillations exhibited a "sheet-like" attractor in Figure 3.7(c). Figure 3.7(d)-(f) show the transition of chaos from type I to type II. A trajectory was going into the center of the former attractor and subsequently spiraling out in Figure 3.7(f). The central point obviously stems from the focus which became unstable by the Hopf bifurcation and after a burst in type II the trajectories returned to the center of the old attractor (type I) along the inset of this saddle focus, *Shil'nikov* chaos [97].

The next-maximum map corresponding to Figure 3.6 and Figure 3.7 are reproduced in Figure 3.8. Period-1 and period-2 potential oscillations correspond to only one and two points in Figure 3.8(a) and (b). Aperiodic potential oscillations (type I) were characterized by a single-maximum map (indicative of a Feigenbaum route) in Figure 3.8(c) [89]. The next-maximum map in Figure 3.8(d)-(f) exhibited a few additional points reflecting the occasional outbursts in the time series. With further reaction time, the bursts become higher, but occurred less and less frequently. This is characteristic for a system approaching a homoclinic orbit (of infinite period).

Each spatiotemporal pattern formation of interfacial potential on the Pt ring electrode is shown in Figure 3.9. Under galvanostatic conditions, spatiotemporal pattern formation of interfacial potential was synchronized due to the global coupling [83].

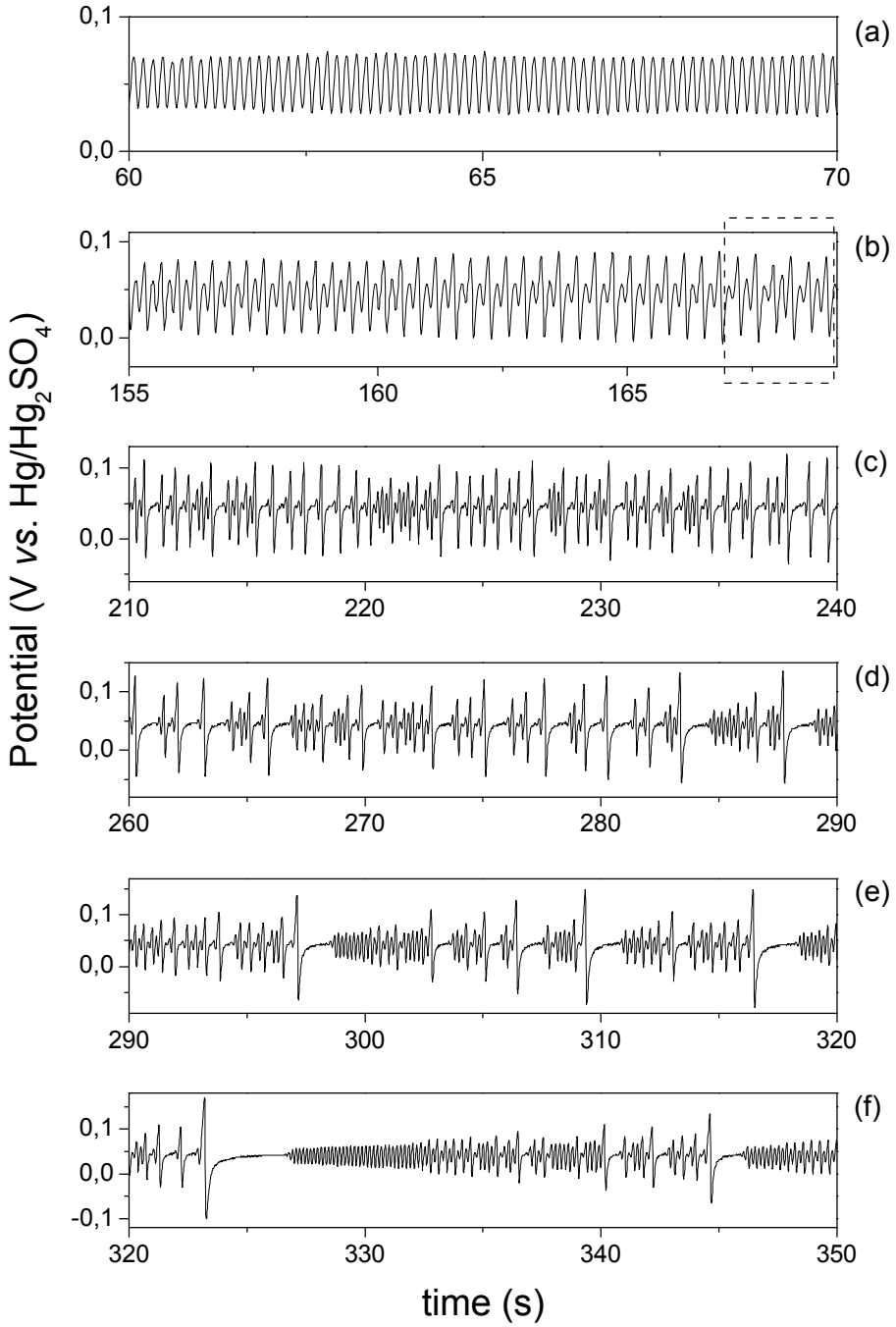

Figure 3.6. Potential oscillations during the oxidation of formic acid in 0.1 M HCOONa/0.033 M H_2SO_4 with 1×10^{-6} M bismuth ions at constant current +53 mA; (a) period-1 oscillations. (b) period-2 oscillations. Dotted box shows the intermediate states (period-2^2) between period-doubling and chaos potential oscillations. (c) chaotic oscillations, (d) and (f) show the changing to the homoclinic (*Shil'nikov*) chaos.

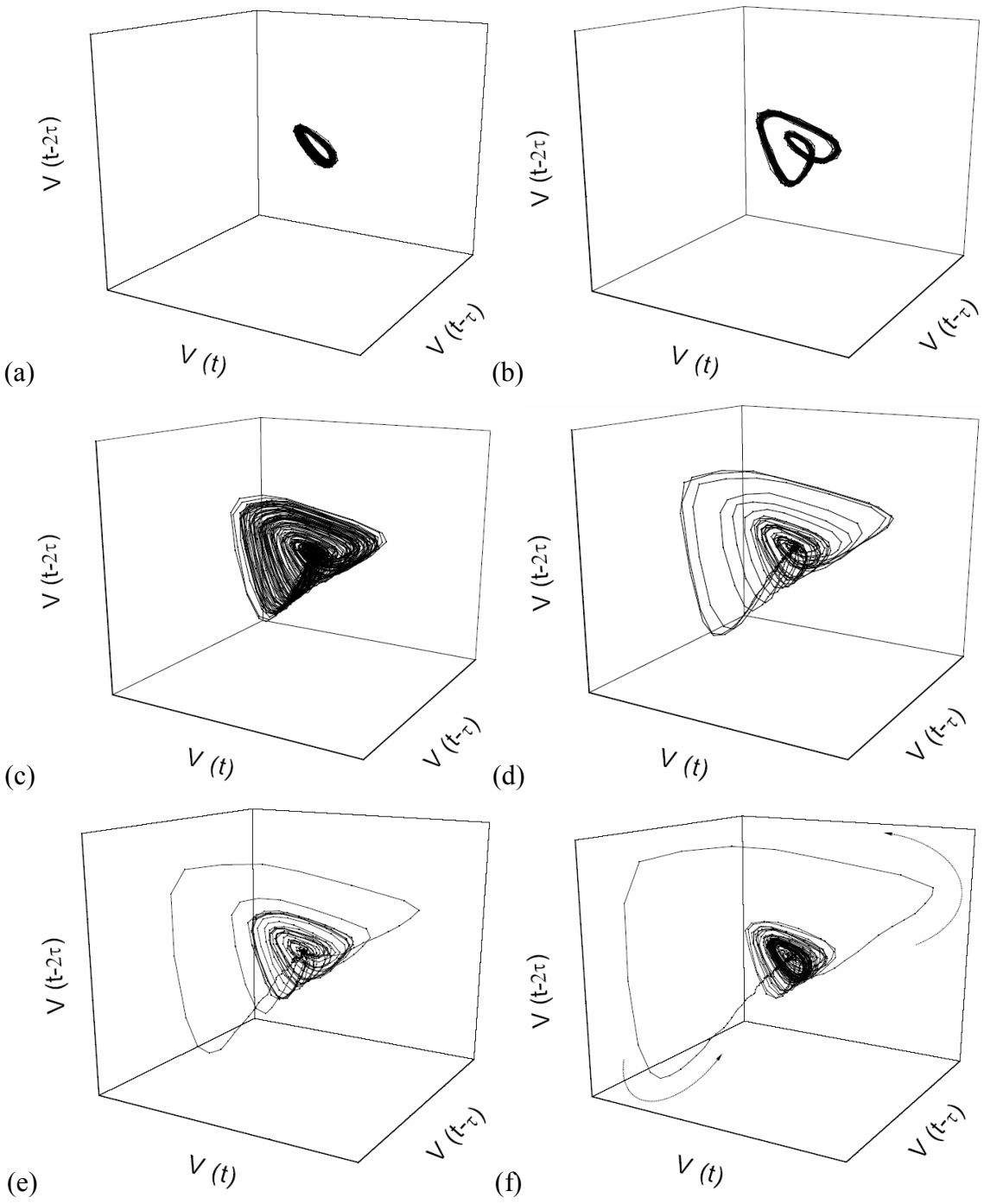

Figure 3.7. Reconstructed attractors obtained from the time series of Figure 3.6.

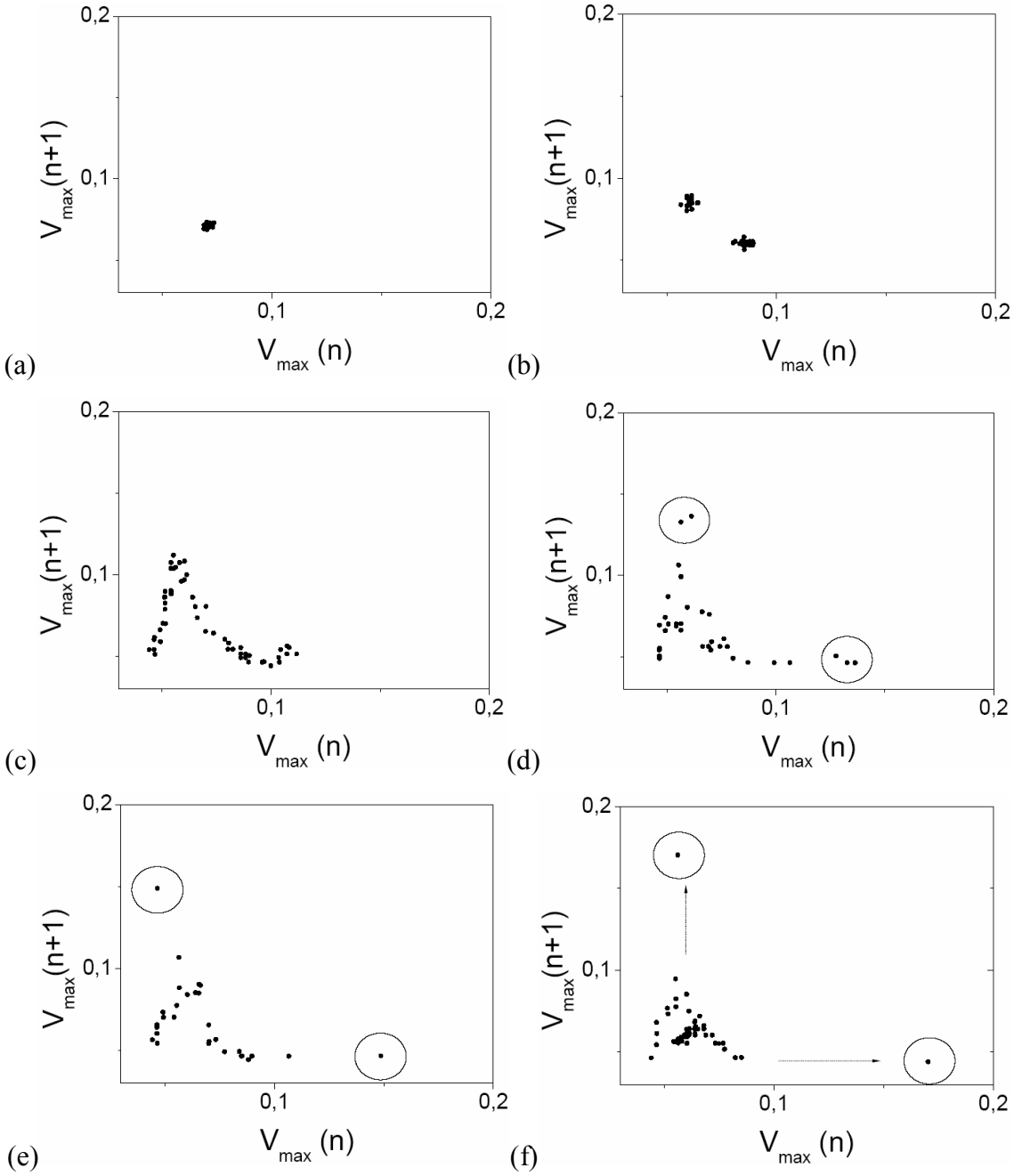

Figure 3. 8. The next-maximum maps obtained from the time series of Figure 3.6. With further reaction time, the bursts occur less frequently, but its strength becomes higher (O: the highest strength of burst)

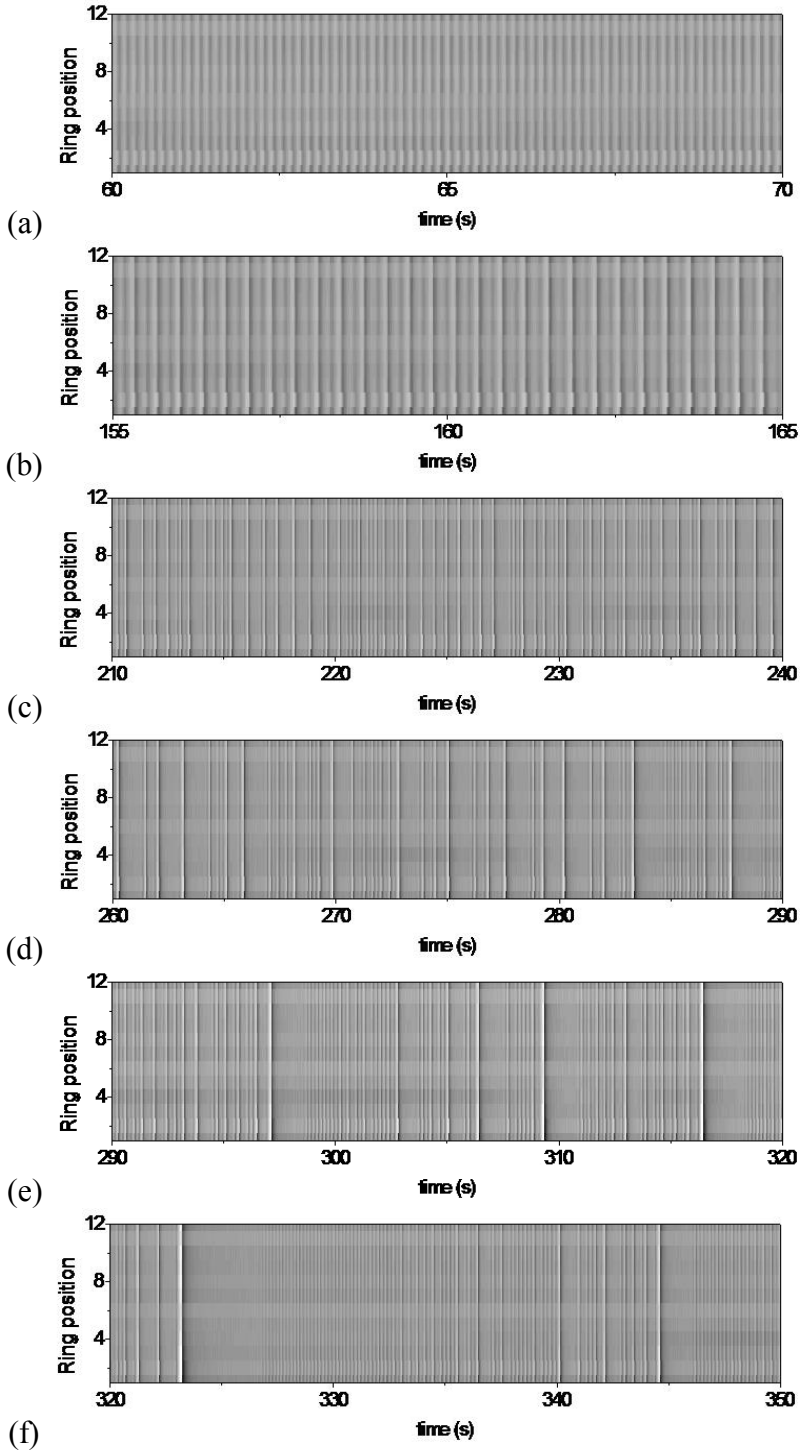

Figure 3.9. Homogeneous spatiotemporal pattern of the interfacial potential as a function of the ring position and time, corresponding to the time series of Figure 3.6. White color corresponds to high interfacial potential.

3.4 Discussion

Although numerous transitions to chaos in electrochemistry have been reported earlier, they mostly involved naturally inhomogeneous electrodes (extended wires, disks) and chaos was explicitly and deliberately shown to be of spatiotemporal nature.

Here we have seen the transition from periodic potential oscillations to *Shil'nikov* chaotic potential oscillations during the formic acid oxidation with bismuth ions *via* a period-doubling route. The attractors and return maps showed no evidence of higher-dimension chaos. The ring electrode is inherently symmetric (all azimuthal position are equivalent) and favors synchronization for galvanostatic conditions. Actually spatial homogeneity was verified in azimuthal direction with potential microprobes. The coherence length is most likely larger than the annulus width; radial inhomogeneity could therefore be excluded on theoretical grounds. The described experiments therefore seem to represent the first clear-out example of purely temporal chaos in an electrochemical experiment.